



HAL
open science

Stability analysis of a socially inspired adaptive voter model

Emmanuel Kravitzch, Yezekael Hayel, Vineeth Varma, Antoine Berthet

► **To cite this version:**

Emmanuel Kravitzch, Yezekael Hayel, Vineeth Varma, Antoine Berthet. Stability analysis of a socially inspired adaptive voter model. *IEEE Control Systems Letters*, 2023, 7, pp.175-180. 10.1109/LC-SYS.2022.3185386 . hal-03608386

HAL Id: hal-03608386

<https://hal.science/hal-03608386v1>

Submitted on 14 Mar 2022

HAL is a multi-disciplinary open access archive for the deposit and dissemination of scientific research documents, whether they are published or not. The documents may come from teaching and research institutions in France or abroad, or from public or private research centers.

L'archive ouverte pluridisciplinaire **HAL**, est destinée au dépôt et à la diffusion de documents scientifiques de niveau recherche, publiés ou non, émanant des établissements d'enseignement et de recherche français ou étrangers, des laboratoires publics ou privés.

Stability analysis of a socially inspired adaptive voter model

Emmanuel Kravitzch¹, Yezekael Hayel¹, Vineeth S. Varma² and Antoine O. Berthet³✉

February 2022

Abstract

In this work, we study an instance of continuous-time voter model over directed graphs on social networks with a specific refinement: the agents can break or create new links in the graph. The edges of the graph thus *co-evolve* with the agents' spin. Specifically, the agents may break their links with neighbours of different spin, and create links with the neighbours of their neighbours (2-hop neighbours), provided they have same spin. We characterize the absorbing configurations and present a particular case that corresponds to a single agent facing two antagonistic ideologies. By asymptotic analysis, we observe two regimes depending on the parameters: in one regime, hesitation disappears rapidly, while when the link creation rate is high enough, slow extinction or *metastability* occurs. We compute the threshold value and illustrate these results with numerical simulations.

1 Introduction

1.1 Research context

Recently, a pronounced surge of interest has grown in control community for the study of *opinion dynamics* in social networks (see for instance [1] and references therein). Among the numerous opinion dynamics' models [2], the Voter Model (VM), pioneered by Thomas Liggett in [3], is probably the most popular. It is a paradigmatic spin system modeling a population of agents each endowed with an orientation (or *spin*) and influence one each others. Soon after its introduction, the VM has been extensively analyzed and refined in various ways. Our

*This work has been completed thanks to the financial support of ANR (National Research Agency) within the project **NiceTweet**: <https://anr.fr/Project-ANR-20-CE48-0009>.

^{†1} Avignon Université, Computer Sciences department (LIA). emmanuel.kravitzch@alumni.univ-avignon.fr and yezekael.hayel@univ-avignon.fr

^{‡2} Research Center for Automatic Control (CRAN), CNRS, Université de Lorraine, France. vineeth.satheeskumar-varma@univ-lorraine.fr

^{§3} Université Paris-Saclay, CNRS, CentraleSupélec, Laboratoire des Signaux et Systèmes (L2S). antoine.berthet@centralesupelec.fr

work is in line with a specific refinement, namely the allowance of network re-configuration performed by the agents themselves. Across social networks, two features are indeed salient: *homophily* and *selective exposure*. They respectively correspond to the natural trend one has to connect with alike people in one hand and dismiss dissonant information on the other hand. By *alike*, we mean having the same spin (which might indicate their preference, orientation or opinion). People influence one another, but the network structure indeed *co-evolves* with the opinion, which in turn influences the opinion dynamics. The more standard VMs over static interaction networks neglect this essential feature of social psychology. The core motivation of this work is then to model and analyze the complex interplay between the node *and* the link dynamics. We thus propose a mathematical framework of opinion-network co-evolution encompassing homophily and selective exposure phenomena. In this work, it is assumed that the linking process is local, i.e., an agent seeks new connections among his 2-hop neighbours. This local linking can be considered to be more realistic compared to a global linking done uniformly at random (u.r) over the total network because it captures a typical search behaviour in the specific context of information-seeking. Several numerical simulations complete the analytical treatment.

1.2 Related work

Since Liggett’s seminal work [3], numerous instances of VMs have been investigated: based on a group-pressure mechanism (called non-linear voter model) [4], using the majority rule [5], or in presence of stubborn agents [6] just to name a few (see the recent survey on VMs [7]). Latterly, the combination of temporal network with VMs –often referred to as *Adaptive* or *Co-evolving* Voter Model (AVM or CVM)– is gaining a lot of attention. Most of the existing papers study a global linking where the agents create new links by picking u.r among the whole population (rewire-to-random) [8], sometimes with an homophilic refinement: rewiring is global u.r but only with agreeing agents (rewire-to-same). In the last two cases, the linking is *long-range*. This u.r linking has also been analyzed in the context of epidemics [9], [10]. In [11] and [12], the linking is also long-range but based on preferential attachment.

Local linking has also been taken into account: in the data-based analysis [13], the authors reveal that locality-constrained link formation substantially shapes the overall network structure. This corroborates the psycho-social studies, where homophily and selective exposure are classical and have been copiously described in the literature: see for instance [14, 15]. The 2-hop-based rewiring, often called *triadic closure* (TC), has thus inspired a generative network model proposed in [16]. Some already existing AVMS also incorporate this important feature: [17] presents an edge-centric model with a mixture of TC and global rewiring. Finally, a combination of non-linear VM and TC has been investigated in [18].

1.3 Contributions

First, to the best of the authors' knowledge, the introduced model is new: a node-centric linear VM combined with pure local linking where breaking and linking are two separated processes, allowing dynamical degree distribution. Second, we take into account the initial configuration and propose an original particular case. Third, as highlighted in [19], the classical issues of VMs like phase transition are often tackled via numerical simulations and approximations. In this work, we propose a detailed mathematical analysis.

1.4 Paper outline

The rest of the paper is organized as follows. In section 2, we introduce our model intertwining edges and nodes' dynamics. In section 3, we characterize absorbing points for $K < \infty$. In Section 4, we focus on a particular scenario where a single agent is under the pressure of two static and opposite blocks and provide an analytical treatment for this case. In Section 5, we display numerical simulations illustrating the results. Section 6 concludes the paper with a discussion on the model and future research perspectives.

2 Model

Let us consider a population of K agents. Each agent is denoted by an integer $k \in [K] := \{1, \dots, K\}$. At each time $t \in \mathbb{R}_+$ each agent k is equipped with a spin $x_k(t) \in \{+1, -1\}$. These two values can represent an orientation, a vote, a preference, etc. Denote by $\vec{x}(t) = (x_1(t), \dots, x_K(t)) \in \{+1, -1\}^K$ the vector of agent's spin at time t . The agents interact through a directed unweighted evolving graph with the associated adjacency matrix $A(t)$, $t \in \mathbb{R}_+$ and $a_{kj}(t) \in \{0, 1\}$. At each time t , each agent k is influenced by its out-neighbours given by the set $N_k(t) := \{j \in [K] : a_{kj}(t) = 1\}$. Note $d_k(t) = |N_k(t)| = (\sum_j a_{kj})(t)$ the out-degree of k at time t , and we write $k \rightarrow_t j$ if there exists a directed path from k to j at time t (the dependence in time will be omitted when clear from the context). The evolution of the network and agent's spin is a Markov Process (\vec{X}, A) with state-space $\mathcal{S} := \{+1, -1\}^K \times \{0, 1\}^{K^2}$. One of the following three types of events can occur and induce a change in the state of the Markov process: a flip of an agent's spin, the creation of a link between two agents or the breaking of an existing link between two agents.

Spin flipping procedure Each agent k owns an individual Poisson "flipping" clock \mathcal{N}_k^ϕ , which means that time duration between two clock ticks are i.i.d and follows $\text{Exp}(\phi)$. At each clock's tick, say at time t , agent k picks an agent j u.r in $N_k(t^-)$. If agent k has a different spin, i.e. $x_j(t^-) \neq x_k(t^-)$, then he aligns on agent j , i.e. $x_k(t) = x_j(t)$. Thus, an interaction between two agents imply that both agents have the same spin after the interaction. The flipping rate $\Phi > 0$ is the rate at which an agent will change his spin value. Note that if

all the neighbours $j \in N_k$ have the same spin as agent k , then the flipping rate of agent k is zero. On the contrary, if all neighbours of agent k have a different spin from that of agent k , then agent k is highly likely to flip soon. This type of jump modelling mimetic behaviour is standard in VMs (see chap. II of [20], [5] or [21] and references therein). In this respect, the numerical value ϕ may be interpreted as the "open-mindedness coefficient" of the epistemic agent.

Definition 1 (Flipping rate) *The flipping rate writes as the following function of the agent, adjacency matrix and spin vector:*

$$\begin{aligned} \Phi : [K] \times \{0, 1\}^{K^2} \times \{-1, 1\}^K &\longrightarrow \mathbb{R}_+, \\ \Phi(k, A, \vec{x}) &= \phi \mathbb{P}(k \text{ picks a disagreeing neighbour}) \\ &= \phi \frac{\sum_j a_{kj} \mathbb{1}_{(x_j \neq x_k)}}{d_k} = \phi \frac{\sum_j a_{kj} (1 - x_k x_j)}{2d_k}. \end{aligned} \quad (1)$$

Link breaking procedure in an analogous way to the previous paragraph, each agent has another Poisson clock, the "link-breaking" clock \mathcal{N}_l^β of parameter β . At each tick of his clock $t \in \mathcal{N}_l^\beta$, agent l picks a neighbour $m \in N_l(t^-)$. If this neighbour has an opposite spin, then the directed link from agent l to agent m is broken. This procedure corresponds to *selective exposure*: the natural trend one has to dismiss dissonant information. This reconfiguration mechanism is also proposed in the context of epidemiology where susceptible nodes cease links with neighbouring infected nodes [9, 10].

Definition 2 (Breaking rate) *The breaking rate B is defined as the rate at which a directed link between two agents breaks, and expressed by the following function:*

$$\begin{aligned} B : [K]^2 \times \{0, 1\}^{K^2} \times \{-1, 1\}^K &\longrightarrow \mathbb{R}_+, \\ B(lm, A, \vec{x}) &= \beta \mathbb{1}_{(x_l \neq x_m)} \mathbb{P}(l \text{ picks } m) \\ &= \beta \underbrace{\mathbb{1}_{(x_l \neq x_m)}}_{\text{selective exposure}} \frac{a_{lm}}{d_l}. \end{aligned} \quad (2)$$

Link creation procedure Finally, new directed links can be created between agents in the network. In the context of *information seeking* [22], we assume the local exploration to prevail on long-range exploration, and then focus only on the former. The 2-hop linking corresponds to iterative search from already known information sources (immediate out-neighbours) to not-yet-explored people. Then, each agent $l \in [K]$ has a third Poisson clock \mathcal{N}_l^γ for exploration and discovery: at each tick of the clock \mathcal{N}_l^γ , agent l seeks new friends among his 2-hop neighbour. For, agent l picks u.r an agent $j \in N_l(t^-)$, and then picks again u.r an $m \in N_j(t^-)$. Finally, agent l creates a directed link toward m provided l is not yet connected to m and the two agents have same spin (homophily). For sake of simplicity, we do *not* assign any social status neither

psychological differentiation to the epistemic agent. Thus, only the spin may distinguish in essence one agent from another, except maybe their respective current network's centrality. This is why the homophily mechanism relies only on the spin differentiation.

Definition 3 (Linking rate) *The linking rate is defined by the function:*

$$\begin{aligned} \Gamma : [K]^2 \times \{0, 1\}^{K^2} \{-1, 1\}^K &\longrightarrow \mathbb{R}_+, \\ \Gamma(lm, A, \vec{x}) &= \gamma \mathbb{1}_{(x_l=x_m)} (1 - a_{lm}) \sum_j \mathbb{P}(l \text{ picks } j) \mathbb{P}(l \text{ picks } m \text{ from } j) \\ \Gamma(lm, A, \vec{x}) &= \underbrace{\gamma \mathbb{1}_{(x_l=x_m)}}_{\text{homophily}} (1 - a_{lm}) \times \sum_j \frac{a_{lj} a_{jm}}{d_l d_j}. \end{aligned} \quad (3)$$

Note that the transition functions Φ , B and Γ do *not* depend on time t , thus defining an *homogeneous* Markov process. These functions completely describe the evolution of the system. Then, the coupled dynamics of the spin profile $\vec{X}(t)$ and the graph $A(t)$ can be written as:

$$\begin{aligned} dX_k &= -2X_k \int_y \mathbb{1}_{(y < p_f(k|A, \vec{x}))} \mathcal{N}_k^\phi(dt dy), \\ da_{lm} &= (1 - a_{lm}) \mathbb{1}_{(x_l=x_m)} \int_y \mathbb{1}_{(y < p_c(lm|A, \vec{x}))} \mathcal{N}_{lm}^\gamma(dt dy) \\ &\quad - a_{lm} \mathbb{1}_{(x_l \neq x_m)} \int_y \mathbb{1}_{(y < p_b(lm|A, \vec{x}))} \mathcal{N}_{lm}^\beta(dt dy), \end{aligned} \quad (4)$$

with

$$p_f(l|A, \vec{x}) = \frac{\sum_j a_{kj} (1 - x_k x_j)}{2d_k}, \quad (5)$$

$$p_b(lm|A, \vec{x}) = \frac{1}{d_l} \text{ and} \quad (6)$$

$$p_c(lm|A, \vec{x}) = \sum_j \frac{a_{lj} a_{jm}}{d_l d_j} \quad (7)$$

and where $\mathcal{N}_k^\phi(dt dy)$, $\mathcal{N}_{lm}^\beta(dt dy)$, and $\mathcal{N}_{lm}^\gamma(dt dy)$ respectively correspond to the flipping, breaking and linking Poisson clocks with intensity $\phi dt \otimes \text{Unif}[0, 1]$, $\beta dt \otimes \text{Unif}[0, 1]$ and $\gamma dt \otimes \text{Unif}[0, 1]$.

3 Characterization of the absorbing states

An interesting state of such a dynamical system is the stationary regime, and in particular, here we also observe absorbing state. If the system reaches such a state, the system gets frozen and does not evolve anymore. In many models, the consensus state where all agents agree is indeed an absorbing state.

The absorbing states are thus of paramount interest for the study of consensus in opinion dynamics. The following proposition describes entirely the set of absorbing states for the Markov process (\vec{X}, A) .

Proposition 4 *Let the set of states \mathcal{A} defined by*

$$\mathcal{A} := \left\{ (\vec{x}, A) \in \mathcal{S} \mid k \rightarrow j \implies a_{kj} = 1 \text{ and } x_k = x_j \right\}.$$

\mathcal{A} is the set of absorbing states of the Markov process (\vec{X}, A) . Furthermore, the set \mathcal{A} is strongly attractive in the sense that there exists a finite time $T_{\mathcal{A}}$ when the Markov process reaches almost surely one of the absorbing states in time, i.e. $T_{\mathcal{A}} := \inf\{t \geq 0 : (X_t, A_t) \in \mathcal{A}\} < \infty$ a.s.

The transient analysis of the dynamics is investigated in the next section when taking a particular initial configuration where one single agent is influenced by two opposite stubborn cliques of large sizes.

4 One single individual under influence

In this particular configuration, the main question is to study how evolves the influence of two opposite stubborn cliques exerted on a single agent when the latter is initially connected to every one of each clique. Thus, we consider a unique agent labeled agent 0 under the influence of two stubborn cliques B^+ and B^- of same sizes : $|B^+| = |B^-| = N$ with $N \gg 1$. Here, the total number of agents in the system is $K = 2N + 1$. Initially, agent 0 is connected to every agent in both cliques, i.e. $a_{0k}(0) = 1$, for all $k \in B^+ \cup B^-$. See Fig. 1 below. We focus only on the links dynamics of agent 0 and its spin evolution. Cliques have fixed complete graph topology and all agents in one clique have the same spin, i.e. for all time t , $a_{lm}(t) = 1$ for all $(l, m) \in (B^+ \times B^+) \cup (B^- \times B^-)$, and $x_j = -1$ (resp. $x_j = +1$) $\forall j \in B^-$ (resp. B^+). Furthermore, the two cliques stay totally disconnected: for all time t , $a_{ml}(t) = a_{lm}(t) = 0 \forall (l, m) \in B^+ \times B^-$. The two blocks B^+ and B^- may correspond to two static opposite ideological mainstreams.

The previous characterization of the absorbing states shows that the spin of agent 0 converges almost surely in finite time toward $\sigma_{\infty} \in \{+1, -1\}$ and in addition agent 0 gets finally connected with all the agents of the final spin and only with them: $a_{0j} = 1$ for all $j \in B^{\sigma_{\infty}}$ and $a_{0i} = 0$ for all $i \in B^{-\sigma_{\infty}}$ in finite time. Nevertheless, depending on the values of the model's parameters, the convergence time may be negligible with respect to K (fast convergence regime) or on the contrary agent 0 may stay hesitant during a time of order a power of K (slow convergence regime, or *metastability*). Our goal is to compute the critical value at which the transition occurs. At each time t , the number of links between agent 0 and each clique is defined as follows:

$$U(t) := \sum_{k \in B^+} a_{0k}(t) \text{ and } V(t) := \sum_{k \in B^-} a_{0k}(t). \quad (8)$$

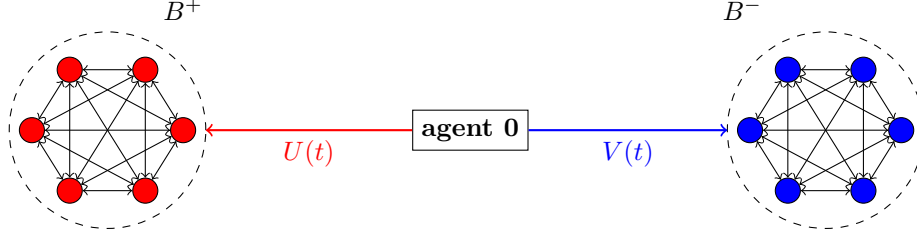


Figure 1: A single agent initially connected to two opposite stubborn cliques of same sizes $|B^+| = |B^-| = 6$.

The spin of agent 0 at each time t is denoted by $X_0(t)$. The stochastic transition rates of the process (U, V, X_0) are described as follows depending on the type of event that occurs and depending on the current spin of agent 0:

$$\begin{aligned}
\Gamma_u(A, \vec{x}) &= \mathbb{1}_{(x_0=+1)} \mathbb{1}_{(U < N)} \gamma \frac{U}{(U+V)} \frac{(N-U)}{N}, \\
B_u(A, \vec{x}) &= \mathbb{1}_{(x_0=-1)} \mathbb{1}_{(U > 0)} \beta \frac{U}{U+V}, \\
\Gamma_v(A, \vec{x}) &= \mathbb{1}_{(x_0=-1)} \mathbb{1}_{(V < N)} \gamma \frac{V}{(U+V)} \frac{(N-V)}{N}, \\
B_v(A, \vec{x}) &= \mathbb{1}_{(x_0=+1)} \mathbb{1}_{(V > 0)} \beta \frac{V}{U+V}, \\
\Phi(A, \vec{x}) &= \phi \frac{\mathbb{1}_{(x_0=-1)} U + \mathbb{1}_{(x_0=+1)} V}{U+V},
\end{aligned} \tag{9}$$

where Γ_u (resp. Γ_v) stands for the upward jump rate of U (resp. V): agent 0 creates a new connection toward B^+ (resp. B^-), and B_u (resp. B_v) corresponds to the downward jump rate of U (resp. V): agent 0 breaks a directed link toward B^+ (resp. B^-). Based on previous transition rates, let us write the associated Stochastic Differential Equations (SDEs):

$$\begin{aligned}
dU(t) &= \int_0^1 \{ \mathbb{1}_{(\gamma y < \Gamma_u)} \mathcal{N}^\gamma(dtdy) - \mathbb{1}_{(\beta y < B_u)} \mathcal{N}^\beta(dtdy) \}, \\
dV(t) &= \int_0^1 \{ \mathbb{1}_{(\gamma y < \Gamma_v)} \mathcal{N}^\gamma(dtdy) - \mathbb{1}_{(\beta y < B_v)} \mathcal{N}^\beta(dtdy) \}, \\
dX_0(t) &= -2X_0(t^-) \int_0^1 \mathbb{1}_{(\phi y < \Phi(A, X))} \mathcal{N}^\phi(dtdy).
\end{aligned} \tag{10}$$

Next analysis of the previous SDEs follows two steps: first, using classical *fluid limit* techniques [23] (see also [24], chap. 9) and different time-scales between links and spin dynamics, the long-term behaviour of the process (U, V) is uncovered; second, a 2-dimensional limiting ODE is used to compute the bifurcation

point of the dynamics.

4.1 Long-term behaviour

Let us define the associated fluid limits as the clique sizes tend to be very large. We consider the following time-space scaled processes for any time t :

$$\begin{aligned}\bar{U}(t) &:= \frac{U(Nt)}{N}, \text{ and } \bar{U}(0) = 1, \\ \bar{V}(t) &:= \frac{V(Nt)}{N}, \text{ and } \bar{V}(0) = 1.\end{aligned}\tag{11}$$

Note that in this time scale, $\bar{X}_0(s) := X_0(Ns)$ oscillates very fast in $\{+1, -1\}$. The system $((\bar{U}, \bar{V}), \bar{X}_0)$ is a slow-fast dynamical system where (\bar{U}, \bar{V}) is "slow" and \bar{X}_0 is "fast". The meaningful quantity in the sequel is rather the *mean dwell time* over any interval $[a, b]$, i.e. the proportion of time agent 0 spin is equal to σ on the interval $[a, b] \subset [0, T]$, defined by the following:

$$\forall \sigma = \pm 1, \quad \int_0^T \mathbb{1}_{[a,b]}(s) L^\sigma(s) ds,$$

with $L^\sigma(s) := \mathbb{1}_{(\bar{X}_0(s)=\sigma)}$. By a slight abuse of notation, we write L^+ instead of L^{+1} . We have the following approximation of the previous coupled SDE.

Proposition 5 (long-term behaviour) *Let T be a finite horizon time. The system (\bar{U}, \bar{V}) can be approximated by the following*

$$\begin{aligned}d\bar{U}(t) &= F_1(\bar{U}, \bar{V})dt + dw_1(t), \\ d\bar{V}(t) &= F_2(\bar{U}, \bar{V})dt + dw_2(t),\end{aligned}\tag{12}$$

with $F = (F_1, F_2) : [0, 1]^2 \rightarrow [0, 1]^2$ the following vector field:

$$\begin{aligned}F_1(u, v) &= \frac{u}{(u+v)^2} (\gamma(1-u)u\mathbb{1}_{(u<1)} - \beta v\mathbb{1}_{(u>0)}) \\ F_2(u, v) &= \frac{v}{(u+v)^2} (\gamma(1-v)v\mathbb{1}_{(v<1)} - \beta u\mathbb{1}_{(v>0)})\end{aligned}\tag{13}$$

and where the noise process (w_1, w_2) decays in some natural norms: $\mathbb{E}\|w_j\|_{[0,T]}^2 \rightarrow 0$ as $N \rightarrow \infty$ for $j = 1, 2$.

Let us first define the intermediate functions:

$$H^+(s) := \frac{\bar{U}}{\bar{U} + \bar{V}}(s) \text{ and } H^-(s) := \frac{\bar{V}}{\bar{U} + \bar{V}}(s),\tag{14}$$

In order to prove the last proposition, let us consider the first term of (10), namely the upward jumps term of U defined by

$$\begin{aligned} U^\uparrow(dt) &:= \int_0^1 \mathbb{1}_{(\gamma y < \Gamma_u)} \mathcal{N}^\gamma(dtdy), \\ U^\downarrow(dt) &:= \int_0^1 \mathbb{1}_{(\beta y < B_u)} \mathcal{N}^\beta(dtdy). \end{aligned} \quad (15)$$

The two other jumps V^\uparrow and V^\downarrow can be treated similarly. The first part of the proof relies on the dwell time approximation to decouple the fast and slow dynamics, as stated in the following lemma.

Lemma 6 *Considering the upward jumps term U^\uparrow , for any $a < b < T$,*

$$\epsilon_{dwe} := \int_0^T \mathbb{1}_{[a,b]}(s) (L^+ - H^+)(s) ds \longrightarrow 0 \text{ as } N \longrightarrow +\infty. \quad (16)$$

The same result is also valid when replacing L^+ and H^+ by L^- and H^- . Moreover, the next result will equally be used.

Lemma 7 *Let us take any bounded process $\{Y_s\}_{s \in [0, T]}$, $\mathcal{N}^\lambda(dtdy) \sim \lambda dt \otimes \text{Unif}[0, 1]$ with $\lambda > 0$ and any $A \subset [0, 1]$. Let $M^\lambda(dtdy) = [\mathcal{N}^\lambda - \lambda \mathbb{1}_{[0, 1]}(y)](dtdy)$. Define for any integer N and $t \in [0, T]$, $\{(Y \mathbb{1}_A) \cdot M\}(Nt) := \frac{1}{N} \int_0^{Nt} \int_y Y_s \mathbb{1}_A(y) M^\lambda(dsdy)$. Then,*

$$\mathbb{E} \|(Y \mathbb{1}_A) \cdot M^\lambda\|_\infty^2 \rightarrow 0 \text{ as } N \rightarrow \infty.$$

With this in mind, we prove the main result.

Proof 8 (of proposition 5) *Let us consider the first term of (10), namely the upward jumps term of U defined by $U^\uparrow(dt)$. Then we have that $dU(t) = U^\uparrow(dt) - U^\downarrow(dt)$.*

The martingale-compensator decomposition for marked point processes ([25], chap.8) applied to \bar{U}^\uparrow gives for all $t \in [0, T]$:

$$\begin{aligned} \bar{U}^\uparrow(t) &= \frac{U^\uparrow(Nt)}{N} = \frac{1}{N} \int_0^{Nt} \int_0^1 \mathbb{1}_{(\gamma y < \Gamma_u)} \mathcal{N}^\gamma(dsdy) \\ &= \frac{1}{N} \int_0^{Nt} \int_y \mathbb{1}_{(\gamma y < \Gamma_u)} [\gamma dsdy + (\mathcal{N}^\gamma(dsdy) - \gamma dsdy)] \\ &= \frac{1}{N} \int_0^{Nt} \Gamma_u(s) ds + \frac{1}{N} \int_0^{Nt} \int_y \mathbb{1}_{(\gamma y < \Gamma_u)} M^\gamma(dsdy) \end{aligned}$$

where $M^\gamma(dsdy) = (\mathcal{N}^\gamma - \gamma \mathbb{1}_{[0, 1]}(y))(dsdy)$ as in lemma 7. By a change of variable and the definition of Γ_u given by equation (9), we get:

$$\frac{1}{N} \int_0^{Nt} \Gamma_u(s) ds = \int_0^t \Gamma_u(Ns) ds = \int_0^t \left(\frac{\bar{U}}{\bar{U} + \bar{V}} (1 - \bar{U}) \right) (s) \mathbb{1}_{(\bar{U} < 1)} L^+(s) \gamma ds,$$

with $L^+(s) = \mathbb{1}_{(X_0(Ns)=+1)}$. We now make use of the dwell time approximation (16):

$$\int_0^t W(s)L^+(s)ds = \int_0^t W(s)H^+(s)ds + \epsilon_{u^\uparrow, dwe},$$

with $W(s) := \left(\frac{\bar{U}}{\bar{U}+\bar{V}}(1-\bar{U})\right)(s)\mathbb{1}_{(\bar{U}<1)}\gamma$ being a bounded process. Therefore, we obtain:

$$\bar{U}^\uparrow(t) = \int_0^t \left(\frac{\bar{U}}{\bar{U}+\bar{V}}\right)^2 (1-\bar{U})\mathbb{1}_{(\bar{U}<1)}\gamma ds + \frac{1}{N} \int_0^{Nt} \int_y \mathbb{1}_{(\gamma y < \Gamma_u)} M^\gamma(dsd y) + \epsilon_{dwe}$$

Applying the same reasoning to \bar{U}^\downarrow , it leads to

$$\bar{U}(t) = \bar{U}^\uparrow(t) - \bar{U}^\downarrow(t) = \int_0^t F_1(\bar{U}, \bar{V})ds + \epsilon_{tot} + \mathcal{M}^N(t),$$

for all $t \in [0, T]$ and where

$$\mathcal{M}^N(t) = \frac{1}{N} \int_0^{Nt} \int_y [\mathbb{1}_{(\gamma y < \Gamma_u)} M^\gamma - \mathbb{1}_{(\beta y < B_u)} M^\beta] (dsd y),$$

and ϵ_{tot} is the aggregate error. It is left to bound the martingale term \mathcal{M}^N standing as the noisy component of the process. Applying lemma 7 to $\mathbb{1}_{(\gamma y < \Gamma_u)} \cdot M^\gamma$ and $\mathbb{1}_{(\beta y < B_u)} \cdot M^\beta$ concludes the proof.

4.2 Bifurcation point

Based on the following proposition we are able to explicitly determine the bifurcation point.

Proposition 9 *Let $g = \frac{\gamma}{\beta}$. For $g < 1$, there is no equilibrium. For $1 < g < 3$, there is a unique equilibrium $p_0 = (w^*, w^*)$ lying on the diagonal, with $w^* = 1 - \frac{1}{g}$ and it is unstable. Finally, for $g > 3$, two extra equilibria p_1, p_2 appear and p_0 becomes stable. In contrast, the two other equilibria p_1, p_2 are always unstable, regardless of the values (γ, β) .*

5 Numerical results

The next picture shows the trajectory of the system $(\bar{U}, \bar{V}) \in [0, 1]^2$ (in green on the picture) with $|B^+| = |B^-| = 500$. The two parabolic curves represent the curves $F_1(x, y) = 0$ and $F_2(x, y) = 0$ in the axis (Ox, Oy) . The intersection points of the last two curves exactly correspond to the equilibria of the system.

In Fig. 2, on the left ($\gamma < 3\beta$), only one equilibrium appears p_0 (the one on the diagonal). Furthermore, it is unstable (not attractive) and the trajectory of the stochastic process is short and quickly gets absorbed. On the other hand

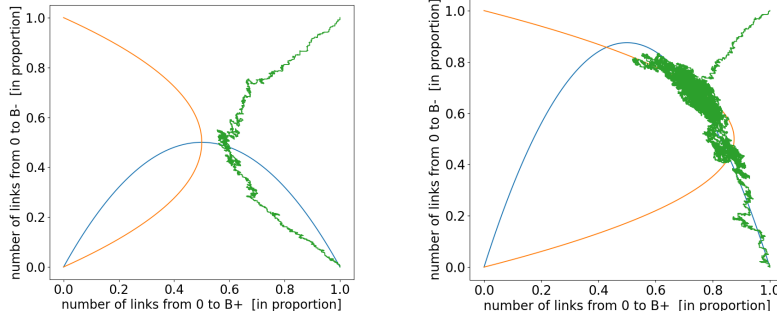


Figure 2: For $\frac{\gamma}{\beta} = 3.5$, persistent hesitation occurs (right). On the contrary, agent 0 is quickly convinced when $\frac{\gamma}{\beta} = 2$ (left). *As expected, the trajectory converges towards a full connection of agent 0 to only one clique.*

when $g > 3$ (as seen on the right), the equilibrium on the diagonal p is attractive. It can be noticed that for all values of β and γ , the two curves cross at $(0, 0)$. This configuration is indeed an (unstable) equilibrium: it corresponds to the case where agent 0 has no link and cannot thus create some anymore. This configuration is actually unreachable provided agent 0 starts with a positive number of out-neighbours. Fig. 3 displays the integral curves associated to the limiting deterministic ODE (13). On the left when $\frac{\gamma}{\beta} = 2$, the instability of the symmetric equilibrium p_0 is patent. While on the right, its attractiveness is easily observable in view of the numerous incoming curves.

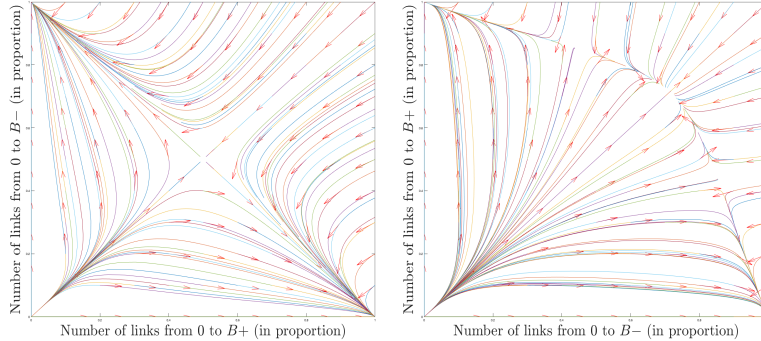


Figure 3: Phase portraits for the two cases $\frac{\gamma}{\beta} = 2$ (left) and $\frac{\gamma}{\beta} = 3.5$. *As expected, the symmetric equilibrium is stable and the 2 other equilibria are unstable in the later case.*

In order to highlight the transition from a fast extinction regime to a *metastable* one, we have plotted in the last figure (see Fig. 4 below) the time (in terms of iterations number which is asymptotically proportional to the continuous time duration) for the system to get absorbed depending on g . For $g < 3$ (subcritical regime), we see that the absorbing time is always very low ($T_{sub} < 2 \times 10^5$).

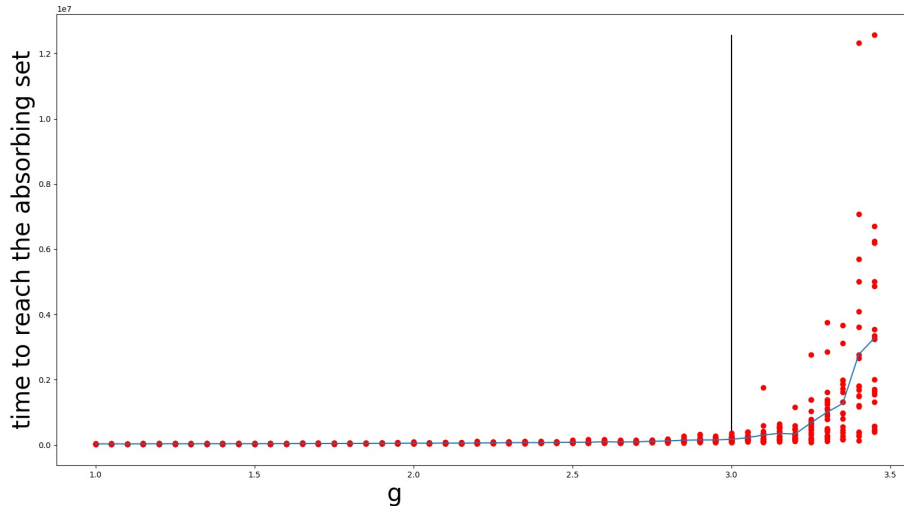


Figure 4: $N = 800$. Each red point corresponds to one simulation. 20 simulations have been performed by step, and the blue curve is the average. The vertical line $g = 3$ corresponds to the critical value.

From $g > 3$ on (super critical), some higher times appear. At $g = 3.1$, a first remarkably high value occurs ($\sim 1.7 \times 10^6 > 8T_{sub}$). And when g gets close to 3.5, the mean value (blue curve) substantially increases, but the extreme values data ($\sim 1.2 \times 10^7 > 60T_{sub}$) are a much stronger indicator of the attractor's emergence .

6 Conclusions and Research perspectives

To conclude, we have presented and analyzed a simple linear adaptive voter model in continuous time whose edges are unweighted and directed with pure local linkage. Though original, it pertains to a flourishing literature on co-evolutionary frameworks. We have used the fluid limits approach to treat a particular case. More generally, adaptive network models may significantly benefit from a mathematical theory of time-varying graphs. In terms of modelling, the multi-layers frame may be able to capture both agents and bounds heterogeneity. Finally, we provide several directions for future work.

Asymmetric case One can generalize the particular case by dropping the assumption $|B^+| = |B^-|$. Setting $|B^-| = q|B^+|$ with $q > 0$ not necessarily equal to 1, the fluid limits analysis still applies, but the bifurcation analysis of the ODE (13) is more involved due to the additional parameter $q > 0$.

Opinion space Defining the structure of the opinion space is a broad and very general problem: continuous or discrete, totally ordered (like an interval) or toric, etc. Though extremely simple, a binary opinion space is quite realistic, since there are many situations where the *choice* has to be made between two possibilities. Nonetheless, the actual opinion may be more complex. Some authors [26, 27] define two layers to distinguish *public* from private opinion, the latter living in a larger and more complex space.

Edge space Concerning the edge space, assigning weights to the edges may add interesting features to the problem, aligning with the reinforcement-penalization mechanism proposed in [28]. Rather than weighting the edges, introducing a qualitative distinction of the links (family, professional, etc) may be another avenue to explore, even though the modeling part seems demanding. Such an additional edge granularity may be harmoniously tailored in accordance with a psycho-social profiling.

Linking mechanism The most structural feature of the present paper is the 2-hop linking procedure (3). Although it may seem natural for modeling iterative search, it assumes the standard agent to be quite conservative. A model *combining* 2-hop linking *and* a specific long-range exploration mechanism like preferential attachment is a plausible candidate for future works.

References

- [1] A. V. Proskurnikov and R. Tempo, “A tutorial on modeling and analysis of dynamic social networks. part i,” Annual Reviews in Control, vol. 43, pp. 65–79, 2017.
- [2] Y. Dong, M. Zhan, G. Kou, Z. Ding, and H. Liang, “A survey on the fusion process in opinion dynamics,” Information Fusion, vol. 43, pp. 57–65, 2018.
- [3] T. M. Liggett and T. M. Liggett, Interacting particle systems. Springer, 1985, vol. 2.
- [4] C. Castellano, M. A. Muñoz, and R. Pastor-Satorras, “Nonlinear q-voter model,” Physical Review E, vol. 80, no. 4, p. 041129, 2009.
- [5] M. E. Yildiz, R. Pagliari, A. Ozdaglar, and A. Scaglione, “Voting models in random networks,” in 2010 Information Theory and Applications Workshop (ITA). IEEE, 2010, pp. 1–7.
- [6] E. Yildiz, A. Ozdaglar, D. Acemoglu, A. Saberi, and A. Scaglione, “Binary opinion dynamics with stubborn agents,” ACM Transactions on Economics and Computation (TEAC), vol. 1, no. 4, pp. 1–30, 2013.
- [7] S. Redner, “Reality-inspired voter models: A mini-review,” Comptes Rendus Physique, vol. 20, no. 4, pp. 275–292, 2019.

- [8] A. Jędrzejewski, J. Toruniewska, K. Suchecki, O. Zaikin, and J. A. Hołyst, “Spontaneous symmetry breaking of active phase in coevolving nonlinear voter model,” Physical Review E, vol. 102, no. 4, p. 042313, 2020.
- [9] S. Trajanovski, D. Guo, and P. Van Mieghem, “From epidemics to information propagation: Striking differences in structurally similar adaptive network models,” Physical Review E, vol. 92, no. 3, p. 030801, 2015.
- [10] D. Guo, S. Trajanovski, R. van de Bovenkamp, H. Wang, and P. Van Mieghem, “Epidemic threshold and topological structure of susceptible-infectious-susceptible epidemics in adaptive networks,” Physical Review E, vol. 88, no. 4, p. 042802, 2013.
- [11] G. Albi, L. Pareschi, and M. Zanella, “On the optimal control of opinion dynamics on evolving networks,” in IFIP Conference on System Modeling and Optimization. Springer, 2015, pp. 58–67.
- [12] —, “Opinion dynamics over complex networks: kinetic modeling and numerical methods,” arXiv preprint arXiv:1604.00421, 2016.
- [13] D. Lee, K.-I. Goh, B. Kahng, and D. Kim, “Complete trails of coauthorship network evolution,” Physical Review E, vol. 82, no. 2, p. 026112, 2010.
- [14] D. Frey, “Recent research on selective exposure to information,” Advances in experimental social psychology, vol. 19, pp. 41–80, 1986.
- [15] M. McPherson, L. Smith-Lovin, and J. M. Cook, “Birds of a feather: Homophily in social networks,” Annual review of sociology, vol. 27, no. 1, pp. 415–444, 2001.
- [16] G. Bianconi, R. K. Darst, J. Iacovacci, and S. Fortunato, “Triadic closure as a basic generating mechanism of communities in complex networks,” Physical Review E, vol. 90, no. 4, p. 042806, 2014.
- [17] N. Malik, F. Shi, H.-W. Lee, and P. J. Mucha, “Transitivity reinforcement in the coevolving voter model,” Chaos: An Interdisciplinary Journal of Nonlinear Science, vol. 26, no. 12, p. 123112, 2016.
- [18] T. Raducha, B. Min, and M. San Miguel, “Coevolving nonlinear voter model with triadic closure,” EPL (Europhysics Letters), vol. 124, no. 3, p. 30001, 2018.
- [19] R. Basu and A. Sly, “Evolving voter model on dense random graphs,” The Annals of Applied Probability, vol. 27, no. 2, pp. 1235–1288, 2017.
- [20] T. M. Liggett et al., Stochastic interacting systems: contact, voter and exclusion processes. Springer science & Business Media, 1999, vol. 324.
- [21] V. Sood, T. Antal, and S. Redner, “Voter models on heterogeneous networks,” Physical Review E, vol. 77, no. 4, p. 041121, 2008.

- [22] S. Pontis and A. Blandford, “Understanding “influence:” an exploratory study of academics’ processes of knowledge construction through iterative and interactive information seeking,” Journal of the Association for Information Science and Technology, vol. 66, no. 8, pp. 1576–1593, 2015.
- [23] R. Darling and J. R. Norris, “Differential equation approximations for markov chains,” Probability surveys, vol. 5, pp. 37–79, 2008.
- [24] P. Robert, Stochastic networks and queues. Springer Science & Business Media, 2013, vol. 52.
- [25] P. Brémaud, Point processes and queues: martingale dynamics. Springer, 1981, vol. 50.
- [26] M. Ye, Y. Qin, A. Govaert, B. D. Anderson, and M. Cao, “An influence network model to study discrepancies in expressed and private opinions,” Automatica, vol. 107, pp. 371–381, 2019.
- [27] V. S. Varma, I.-C. Morărescu, and Y. Hayel, “Continuous time opinion dynamics of agents with multi-leveled opinions and binary actions,” in IEEE INFOCOM 2018-IEEE Conference on Computer Communications. IEEE, 2018, pp. 1169–1177.
- [28] A. A. Santos, S. Kar, R. Krishnan, and J. M. Moura, “Strong attractors in stochastic adaptive networks: Emergence and characterization,” arXiv preprint arXiv:1605.09450, 2016.
- [29] D. A. Levin and Y. Peres, Markov chains and mixing times. American Mathematical Soc., 2017, vol. 107.
- [30] J.-F. Le Gall et al., Brownian motion, martingales, and stochastic calculus. Springer, 2016, vol. 274.

A Appendix

A.1 Proof of proposition 4 (absorbing states)

Proof 10 *We first show that all configurations in \mathcal{A} are absorbing. Let us take $(\vec{x}, A) \in \mathcal{A}$. It suffices to show that all rates are identically 0. Let $l, m \in [K]$. There are two cases:*

- *either $l \rightarrow m$. In this case, $a_{lm} = 1$ and thus $\Gamma(lm, \vec{x}, A) = 0$. We also have $x_l = x_m$, implying $B(lm, \vec{x}, A) = 0$.*
- *or $\neg(l \rightarrow m)$. In this case, $a_{lm} = 0$ and thus $B(lm, \vec{x}, A) = 0$. Moreover, there is obviously no path of size 2 between l and m , which implies: $a_{lj}a_{jm} = 0 \forall j \implies \Gamma(lm, \vec{x}, A) = 0$.*

We now show that the flip rate is identically 0: let us take $k \in [K]$. For all $j \in N_k^{\text{out}}, j \rightarrow k \implies x_k = x_j \implies \Phi(k, \vec{x}, A) = 0$.

We have shown that all elements of \mathcal{A} are absorbing. We shall show that they are the only ones: let us take a configuration $(\vec{x}, V) \notin \mathcal{A}$. It means that there exists some $k, j \in [K]$ with $k \rightarrow j$ and such that $(x_k \neq x_j \text{ or } a_{kj} = 0)$. Then, it exists a directed path $p = p_1 p_2 \dots p_M$ of size M such that $p_1 = k, p_M = j$ and $a_{p_l p_{l+1}} = 1$.

We define the index v as $v := \min\{l \in [2, M] : (x_{p_l} \neq x_{p_{l-1}} \text{ or } a_{p_l p_{l-1}} = 0)\}$. This set is finite and non empty because it contains M . The minimum necessarily exists and we have: $x_{p_{l-1}} = x_k, a_{k p_{l-1}} = 1$ and $a_{p_{l-1} p_l} = 1$. Here, we have two cases:

- If $x_{p_l} \neq x_k$, then p_{l-1} is susceptible to flip: $\Phi(p_{l-1}, \vec{u}, V) > 0$. This configuration is thus not absorbing.
- Else, $x_{p_l} = x_{p_{l-1}} = x_k$ but $a_{k p_l} = 0$. In this case, k is thus susceptible to get linked with p_l : $\Gamma(k p_l, \vec{x}, V) > 0$.

Finally, the finite time convergence is an immediate corollary on the following lemma:

Lemma 11 Let a discrete-time Markov chain $\{(X_k)_k, Q_{xy}\}$ in a finite state space $S = S' \cup \partial$ with S' being a SCC and ∂ an absorbing state. If it exists an $s \in S'$ such that $p_{s\partial} > 0$, then a.s the Markov chain is absorbed in finite time.

Proof 12 (of lemma 11) We shall show that the hitting time of ∂ T_∂ is integrable.

$$\begin{aligned} \mathbb{E}_x[T_\partial] &\leq \mathbb{E}_x T_s + \sum_k \mathbb{E}_s \left\{ \mathbb{1}\{X \text{ hits } k \text{ times } s \text{ and jumps to } \partial\} \times (T_s^{(k)} + 1) \right\} \\ &\leq \mathbb{E}_x T_s + \mathbb{E}_s \sum_k T_s^{(k)} \mathbb{1}\{Z = k\}, \end{aligned}$$

where $T_s^{(k)}$ is the k^{th} hitting time of s , and Z is a geometric law with a success probability $Q_{s\partial}$. Because $\mathbb{E}_s T_s^{(k)} = k \mathbb{E}_s T_s$, we have,

$$\mathbb{E}_x T_\partial \leq \mathbb{E}_x T_s + \sum_k k \mathbb{E}_s T_s (1 - Q_{s\partial})^k Q_{s\partial} < \infty.$$

$\mathbb{E} T_\partial < \infty$ implies $\mathbb{P}(T_\partial < \infty) = 1$.

One has finally to notice that for all $(x, A) \in \mathcal{S} : (x, A) \rightarrow \mathcal{A}$. Applying the lemma to the embedded Markov chain terminates the proof.

A.2 Proof of lemma 6 (dwell-time approximation)

Proof 13 To prove this, let us define a subdivision of $[a, b]$ $\Delta := \{a = t_1 < \dots < t_p = b\}$ with $I_j = [t_j, t_{j+1}[$ and $|\Delta| = \max_j |I_j|$. Consider the approximation

$\tilde{H}^\sigma(s) := \sum_j H^\sigma(t_j) \mathbb{1}_{I_j}(s)$ and the approximation \tilde{L}^σ as the locally homogeneous Markov: on I_j , its transition rates are $\rho_{0 \rightarrow 1} = \phi H^\sigma(t_j)$, and $\rho_{1 \rightarrow 0} = \phi H^{-\sigma}(t_j)$ whose unique stationary probability measure is $(H^\sigma(t_j), H^{-\sigma}(t_j))$. We then write

$$\int (L^\sigma - H^\sigma) = \int (\tilde{L}^\sigma - \tilde{H}^\sigma) + \int (\tilde{H}^\sigma - H^\sigma) + \int (L^\sigma - \tilde{L}^\sigma). \quad (17)$$

As N gets large, the convergence to 0 of the first term in the right-hand side of (17) is an application of the ergodic theorem (sect. 4.7 of [29]): a.s., $\forall j = 1, \dots, p, \exists N_{\epsilon, j}$ such that $\forall N > N_{\epsilon, j}$, we have

$$\begin{aligned} & \int_{I_j} (\tilde{L}^\sigma(Ns) - H^\sigma(t_j)) ds < \epsilon \\ \implies & \exists N_\epsilon \perp j, \int_{[a, b]} (\tilde{L}^\sigma - \tilde{H}^\sigma) = \sum_{j=1}^p \int_{I_j} (\tilde{L}^\sigma - \tilde{H}^\sigma) < \epsilon p. \end{aligned}$$

As N gets large, the second term of (17) vanishes as well since on each interval I_j , H^σ varies about $(\beta + \gamma)|\Delta|$:

$$\begin{aligned} \sup_{s \in I_j} |\tilde{H}^\sigma(s) - H^\sigma(Ns)| & \leq \left| \{ \text{jumps on } [Nt_j, Nt_{j+1}] \} \right| \times (\text{jump size}) \\ & \leq (|\mathcal{N}^{\gamma N}| + |\mathcal{N}^{\beta N}|) (I_j) \frac{1}{N}. \end{aligned}$$

Applying Tchebychev inequality on the random variables $|\mathcal{N}^{\lambda N}|(I_j)$ which are Poisson distributions with parameter $\lambda N |I_j|$ for $\lambda \in \{\beta, \gamma\}$:

$$\forall \eta, j, \mathbb{P} \left(\left| \frac{|\mathcal{N}^{\lambda N}|(I_j)}{N} - |I_j| \lambda \right| > \eta \right) \leq \frac{\lambda |I_j|}{\eta^2 N} \rightarrow 0 \text{ as } N \rightarrow \infty.$$

As the intervals I_j are disjointed, the random variables $|\mathcal{N}^{\gamma N}|(I_j)$ are independent for all $\epsilon > 0$,

$$\begin{aligned} \mathbb{P} \left(\int_0^T \mathbb{1}_{[a, b]} |H^\sigma - \tilde{H}^\sigma|(Ns) > \epsilon \right) & \leq \mathbb{P} \left(|b - a| \sup_{a < s < b} |H^\sigma - \tilde{H}^\sigma|(Ns) > \epsilon \right) \\ & \leq 1 - \prod_{j=1}^p \mathbb{P} \left(\sup_{s \in I_j} |H^\sigma - \tilde{H}^\sigma|(Ns) < \frac{\epsilon}{b - a} \right) \\ & \leq 1 - \prod_{j=1}^p \left(1 - \frac{\gamma |I_j|}{\epsilon_0^2 N} \right) < 1 - \left(1 - \frac{\gamma |\Delta|}{\epsilon_0^2 N} \right)^p \rightarrow 0 \end{aligned}$$

as $N \rightarrow \infty$.

Finally, we shall show that the last term $\int_{I_j} (L^\sigma - \tilde{L}^\sigma)$ tends to 0:

$$\mathbb{E} \int_{I_j} (L^\sigma - \tilde{L}^\sigma) = \int_{s \in I_j} \int_{x=+1, -1} \mathbb{1}_{(x=\sigma)} (\mu_s - \tilde{\mu}_s)(dx) ds,$$

where μ_s (resp. $\tilde{\mu}_s$) stands for the law at time s of the spin X^0 of agent 0 (resp. \tilde{X}_0). $\{\tilde{\mu}_s\}_{s \in I_j}$ only depends on $H^{\pm\sigma}(t_j)$ while μ_s continuously depends on (U, V) . By the computations performed before, their difference is of order $|\Delta|$, implying

$$\begin{aligned} & \left| \mathbb{E} \int_{I_j} (L^\sigma - \tilde{L}^\sigma) \right| \leq |I_j| \sup_{s \in I_j} |\mu_s - \tilde{\mu}_s| < |I_j| (|\Delta| \gamma), \\ \implies & \mathbb{E} \int \mathbb{1}_{[a,b]} (L^\sigma - \tilde{L}^\sigma) = \mathbb{E} \sum_j \int_{I_j} (L^\sigma - \tilde{L}^\sigma) \leq T |\Delta|. \end{aligned}$$

A.3 Proof of lemma 7 (convergence of the martingale term)

Proof 14 We have:

$$\begin{aligned} \mathbb{E} \left\{ (Y \mathbb{1}_A) \cdot M^\lambda \right\}^2 (Nt) &= \frac{1}{N^2} \mathbb{E} \left\{ \int_0^{Nt} \int_y Y_s \mathbb{1}_A(y) M^\lambda(dsdy) \right\}^2 \\ &= \frac{|A|^2}{N^2} \mathbb{E} \left\{ \int_0^{Nt} Y_s [\mathcal{N}^\lambda - \lambda](ds) \right\}^2 \\ &= \frac{|A|^2}{N^2} \mathbb{E} \int_0^{Nt} Y_s^2 \langle \mathcal{N}^\lambda - \lambda \rangle (ds), \end{aligned}$$

where the last equality is due to the Moments formula (eq. (5.8) of [30]), and where $\langle \cdot \rangle$ (resp. $\langle \cdot, \cdot \rangle$) stands for the quadratic variation (resp. co-variation). Because the family of processes $\{Y_s(w) \mathbb{1}_A : Y_s \text{ bounded, } A \subset [0, 1]\}$ generates all the bounded processes $Z_s(w, y) : [0, T] \times \Omega \times [0, 1] \rightarrow \mathbb{R}$, it can be straightforwardly extended to the latter space. Moreover, by standard properties on quadratic variations, namely $\langle \mathcal{N}^\lambda \rangle = \mathcal{N}^\lambda$ and $\langle \lambda \rangle = \langle \mathcal{N}^\lambda, \lambda \rangle = 0$, we get

$$\langle \mathcal{N}^\lambda - \lambda \rangle = \langle \mathcal{N}^\lambda \rangle + \langle \lambda \rangle - 2\langle \mathcal{N}^\lambda, \lambda \rangle = \mathcal{N}^\lambda.$$

It finally leads to

$$\begin{aligned} \mathbb{E} \| (Y \mathbb{1}_A) \cdot M^\lambda \|^2_\infty &= \mathbb{E} \sup_{0 < t < T} |(Y \mathbb{1}_A) \cdot M^\lambda|^2 (Nt) \\ &\leq \mathbb{E} |(Y \mathbb{1}_A) \cdot M^\lambda|^2 (NT) \\ &\leq \frac{|A|^2}{N^2} \mathbb{E} \int_0^{Nt} Y_s^2 \mathcal{N}^\lambda(ds) \\ &= \frac{|A|^2}{N^2} \int_0^{Nt} \mathbb{E}[Y_s^2] \lambda(ds) \\ &\leq |A| T \|Y\|_\infty^2 \lambda \frac{1}{N} \rightarrow 0 \text{ as } N \rightarrow \infty. \end{aligned}$$

A.4 Proof of proposition 9 (bifurcation point of the limiting ODE)

Proof 15 Recall $g = \frac{\gamma}{\beta}$. Let find a couple $(u, v) \in [0, 1]^2$ solution of the following system:

$$\begin{cases} F_1(u, v) = 0 \\ F_2(u, v) = 0 \end{cases} \iff \begin{cases} \gamma(1-u)u - \beta v = 0 \\ \gamma(1-v)v - \beta u = 0 \end{cases}$$

The first equation gives that $v = g(1-u)u$, and by substitution, the second equations leads to:

$$g^3 z^3 - g^3 z^2 + g^2 z - 1 = 0,$$

where $z = 1 - u$. We factorize the last expression by the solution $z = \frac{1}{g}$, that gives:

$$g^2 \left(z - \frac{1}{g} \right) (gz^2 - (g-1)z + g^{-1}) = 0. \quad (18)$$

Note that this solution is symmetric, if $u = 1 - \frac{1}{g}$ then $v = 1 - \frac{1}{g}$ from first equation of the system. Focus now on the second degree equation $gz^2 - (g-1)z + g^{-1} = 0$. Let us compute its discriminant Δ :

$$\Delta = (g+1)(g-3).$$

Then depending on the value of g , different solutions occur for equation (18) on the interval $]0, 1[$:

- if $0 < g < 1$, then there is no solution for equation (18) on the interval $]0, 1[$,
- if $1 \leq g < 3$, there exists a unique solution $z^* = \frac{1}{g}$,
- else if $g > 3$, there are three different solutions:

$$z^* = \frac{1}{g}, \quad z_0^* = \frac{g-1 - \sqrt{(g+1)(g-3)}}{2g}, \quad \text{and}$$

$$z_1^* = \frac{g-1 + \sqrt{(g+1)(g-3)}}{2g}.$$

We now study the stability of the symmetric equilibria $u^* = v^* = 1 - \frac{1}{g}$ when $g > 1$.

$F: (u, v) \in]0, 1[^2 \rightarrow F(u, v) \in]0, 1[^2$ is of the form $D(u, v) \cdot \bar{F}(u, v)$, where $D = \begin{bmatrix} d_1(u, v) & 0 \\ 0 & d_2(u, v) \end{bmatrix} = \begin{bmatrix} \frac{u}{(u+v)^2} & 0 \\ 0 & \frac{v}{(u+v)^2} \end{bmatrix}$ is a diagonal matrix and

$$\bar{F}(u, v) = \begin{bmatrix} \gamma(1-u)u & -\beta v \\ -\beta u & \gamma(1-v)v \end{bmatrix}.$$

Whence

$$\partial F = (\partial D).\bar{F} + D.(\partial\bar{F})$$

Because we study the derivative only at equilibrium, we get $F = \bar{F} = 0$. The first term in the product derivative thus vanishes. It is left to compute the second one. First, $\partial\bar{F}_{(u,v)} = \begin{bmatrix} \gamma(1-2u) & -\beta \\ -\beta & \gamma(1-2v) \end{bmatrix}$. Then, compute the spectrum of the normalized (divided by β) linearization:

$$\begin{aligned} \chi(\lambda) &= \det \left(\frac{1}{\beta} D.(\partial\bar{F}) - \lambda I_{2 \times 2} \right) \text{ for } \lambda \in \mathbb{R}, \\ &= \det(D) \times \det \left(\frac{1}{\beta} \partial\bar{F} - D^{-1}\lambda \right) \\ &= \det(D) \times \begin{vmatrix} g(1-2u) - \frac{\lambda}{d_1} & -1 \\ -1 & g(1-2v) - \frac{\lambda}{d_2} \end{vmatrix}, \\ &\propto \left(g(1-2u) - \frac{\lambda}{d_1} \right) \left(g(1-2v) - \frac{\lambda}{d_2} \right) - 1, \\ &\propto \frac{1}{d_1 d_2} \lambda^2 - g \left\{ \frac{(1-2v)}{d_1} + \frac{(1-2u)}{d_2} \right\} \lambda \\ &\quad + g^2(1-2u)(1-2v) - 1. \end{aligned}$$

Taking $\chi(\lambda) = 0$ is equivalent to

$$\begin{aligned} &\lambda^2 - g \{ (1-2v)d_2 + (1-2u)d_1 \} \lambda \\ &\quad + g^2(1-2u)(1-2v)d_1 d_2 - d_1 d_2 \\ &= \lambda^2 - g(A+B)\lambda + g^2 AB - d_1 d_2 = 0, \text{ where} \\ &A = (1-2v)d_2, B = (1-2u)d_1 \text{ and} \\ &\Delta = g^2(A-B)^2 + 4d_1 d_2 > 0. \end{aligned}$$

Then, the eigenvalues λ^- and λ^+ are:

$$\lambda^- = \frac{g(A+B) - \sqrt{g^2(A-B)^2 + 4d_1 d_2}}{2}$$

and

$$\lambda^+ = \frac{g(A+B) + \sqrt{g^2(A-B)^2 + 4d_1 d_2}}{2}.$$

For the symmetric equilibrium to be attractive, the eigenvalues must be negative, meaning that $\lambda_+ < 0$. It gives the two conditions:

$$\begin{aligned} &g(A+B) + \sqrt{g^2(A-B)^2 + 4d_1 d_2} < 0 \iff \\ &A+B < 0 \text{ and } (A+B)^2 > (A-B)^2 + \frac{4d_1 d_2}{g^2} \end{aligned}$$

The first condition gives:

$$A + B < 0 \iff (1 - 2v)d_2 + (1 - 2u)d_1 < 0.$$

But, as we are looking at the symmetric equilibrium point $u = v = 1 - \frac{1}{g}$, then $d_1 = d_2$. Thus,

$$A + B < 0 \iff g > 2.$$

The second condition is more restrictive:

$$\begin{aligned} (A + B)^2 &> (A - B)^2 + \frac{4d_1d_2}{g^2} \\ \iff AB &> \frac{d_1d_2}{g^2} \\ \iff (1 - 2(1 - \frac{1}{g}))^2 &> \frac{1}{g^2}. \end{aligned}$$

Here there are two cases: either $1 - 2(1 - \frac{1}{g}) > \frac{1}{g}$; after simple computations, it leads to $g < 1$ which is not admissible because of the last inequality. Only remains the other possibility: $1 - 2(1 - \frac{1}{g}) < -\frac{1}{g}$, leading to $g > 3$.

To conclude, when $g > 3$ then the symmetric equilibrium $u = v = 1 - \frac{1}{g}$ is a stable equilibrium of the approximated dynamics.